Formation of cobalt disilicide films on $(\sqrt{3}\times\sqrt{3})6H$-SiC(0001)

W. Platow, D. K. Wood, K. M. Tracy, J. E. Burnette, R. J. Nemanich, and D. E. Sayers
Department of Physics, North Carolina State University, Raleigh, North Carolina 27695-8202
(Received 22 August 2000; published 1 March 2001)

This paper presents a detailed study of thin Co films grown directly, sequentially, and by codeposition with Si on the $(\sqrt{3}\times\sqrt{3})$-$R30°$ surface of $6H$-SiC(0001). The structure, chemistry, and morphology of the films were determined using x-ray absorption fine structure, x-ray photoelectron spectroscopy, Auger electron spectroscopy, and atomic force microscopy. For directly deposited Co films (1–8 nm) graphite layers form on top of the film surface during annealing, whereas Co stays mainly unreacted over a temperature range of 300–1000 °C. The formation of $CoSi_2$ is achieved by sequential and codeposition of Co and Si. Films annealed at 550 °C are polycrystalline and further annealing to 650 °C causes no C segregation, but there is islanding of the films. Attempts to improve film morphology and homogeneity including applying a template method and varying growth temperature are also reported.

DOI: 10.1103/PhysRevB.63.115312 PACS number(s): 68.55.Jk, 81.15.−z, 68.55.Nq

I. INTRODUCTION

The physical and electronic properties of silicon carbide (SiC) make it an important semiconductor material for short-wavelength optoelectronic, high-temperature, radiation-resistant, and high-power/high-frequency electronic devices.[1] Cobalt disilicide ($CoSi_2$) is considered a promising electrical contact material to SiC due to its low resistivity and good thermal stability. Recent Co/SiC thin-film studies investigated their electrical[2–6] and structural properties.[5–7] Mostly, directly deposited Co films,[2,6–9] but also thick Si/Co/SiC bilayers (126.5 nm Si/50 nm Co), were studied.[3,4] For directly deposited Co films the formation of cobalt monosilicide (CoSi) and graphite was observed,[6] and unreacted Co metal was reported[7] for annealing at temperatures up to 800 °C. Sequentially deposited thick Si/Co bilayers annealed at 900 °C are reported to form columnar grains of $CoSi_2$ with no graphite segregation.[5]

The properties of Ohmic contacts and the electrical characteristics of Schottky barrier diodes are very sensitive to surface preparation techniques and can depend strongly on the surface cleaning procedure used prior to forming the contact. Relatively little attention has been paid to the different SiC surface reconstructions before depositing the metal films although these may affect the nucleation process during the formation of $CoSi_2$ as well as the uniformity, flatness, and stoichiometry of the interface. Most studies of the electrical behavior of cobalt and cobalt silicide contacts to SiC have reported using only a wet chemical cleaning procedure prior to doing metallization.[2–5] Results have established that the (1×1) surface obtained after wet chemical cleaning procedures contains oxygen,[10] which can decrease the metal adhesion, enhance the specific contact resistance, affect Schottky barrier heights, and create electrically active defects that may change the transport of electrons or holes through the contact. On the other hand, the Si-rich (3×3) surface reconstruction obtained by *in situ* chemical vapor cleaning results in the formation of 0.3-μm-high Si islands[11] and therefore may create inhomogeneities at the interface to the metal contact. In a previous study by our group, low-energy electron diffraction (LEED) patterns were measured after thermal desorption in ultahigh vacuum (UHV) and prior to deposition of Co films, showing a (1×1) surface reconstruction.[7] However, directly deposited Co films (2.5 and 10 nm) annealed at 500 and 800 °C contain unreacted cobalt metal.

In this work we focus on the Si-terminated (0001) surface of $6H$-SiC with the $(\sqrt{3}\times\sqrt{3})$-$R30°$ surface reconstruction. When carefully prepared, this surface is clean, and contains no surface contamination such as oxygen. It is well ordered, with $\frac{1}{3}$ atomic layer of additional Si atoms,[12] i.e., it is slightly Si rich, and accumulates no Si islands. As will be shown in Sec. III, formation of thin $CoSi_2$ films can be achieved by sequential and codeposition of Co and Si followed by annealing at 550 °C. We describe in detail the effects of higher annealing temperatures, variation of growth temperature, and use of template layers.

II. EXPERIMENTAL DETAILS

The Co films were directly, sequentially, and codeposited with Si on $6H$-SiC(0001) wafers in an UHV system that has a base pressure in the 10^{-10} Torr range, allowing *in situ* transfer between facilities for molecular beam epitaxy, low-energy electron diffraction, Auger electron spectroscopy (AES), and x-ray photoelectron spectroscopy (XPS). The $6H$-SiC(0001) wafers (silicon face) were *n* type and purchased from CREE Research Inc. A tungsten film of several micrometers thickness was sputtered onto the back side of each wafer to facilitate *in situ* heating by absorption of infrared radiation. After exposure to UV/ozone irradiation for 10 min the wafers were chemically etched with a $HF:H_2O$:ethanol (1:1:10) solution for another 10 min. This procedure was repeated with exposure and etching times of 5 min. The wafer was then mounted on a molybdenum sample holder and loaded into the vacuum system. The surface was prepared by *in situ* thermal desorption at 1200 °C for 15 min under Si flux of 0.003 nm/s, resulting in a $(\sqrt{3}\times\sqrt{3})$-$R30°$ SiC surface reconstruction as determined by LEED. Co (1–8 nm) and Si (3.6–29.2 nm) films were then deposited using a Si:Co weight ratio of 3.64, which is the stoichiometric ratio for $CoSi_2$. The films were subsequently annealed at various temperatures in the range of 300–1200 °C for 20

min. The temperature was measured using an optical pyrometer. The deposition was controlled with quartz crystal thickness monitors calibrated with profilometry and atomic force microscopy (AFM). No surface contamination was found for the $(\sqrt{3}\times\sqrt{3})$ SiC surface reconstruction and after film deposition within the AES and XPS detection limit [$<\frac{1}{10}$ monolayer (ML)]. The XPS system consists of a Clam II hemispherical electron energy analyzer with a radius of 100 mm. The Al $K\alpha$ (1486.6 eV) x-ray source was operated at 13 kV with an emission-controlled current of 20 mA.

The annealed films were characterized *ex situ* with x-ray absorption fine structure (XAFS) and atomic force microscopy. XAFS data were collected at room temperature in the fluorescence mode with a Canberra 13-element Ge detector at the Co *K* edge (7709 eV) at beamline X-11A at the National Synchrotron Light Source. The incident photon beam was monochromatized with a double-crystal Si(100) monochromator detuned 30% to suppress higher harmonics. Energy calibration was set to 7709 eV at the Co foil *K* edge inflection point. XAFS data analysis was performed with the MACXAFS 4.1 package.[13] Fourier transforms of k_2-weighted XAFS data were done over the wave-vector range $k=3.5-10.3\,\text{Å}^{-1}$ after preedge subtraction, normalization, background removal, and conversion from energy scale to wave vector *k*. AFM data were acquired in contact mode with a Park Scientific Autoprobe M5 instrument (typical radius of curvature of the AFM silicon nitride tips is about 10 nm).

III. RESULTS AND DISCUSSION

A. Direct deposition

The annealing dependence of AES spectra for 8 nm Co directly deposited onto $(\sqrt{3}\times\sqrt{3})$ SiC together with the data for the clean $(\sqrt{3}\times\sqrt{3})$-$R30°$6*H*-SiC(0001) surface are depicted in Fig. 1. All scans were obtained with the sample at room temperature, and the annealing steps were for 10 min at temperatures up to 700 °C. The $(\sqrt{3}\times\sqrt{3})$ reconstruction [Fig. 1(a)] is oxygen free within the AES detection limit and gives a peak-to-peak intensity Si/C ratio of 2.48 that is comparable to the ratio of 2.21 given by Starke, Schardt, and Franke for the same reconstruction.[14] Our measurements show that this ratio can vary up to 3.0 depending on the Si flux during the thermal desorption. This is in agreement with other studies[15–17] in which silicon-rich as well as carbon-rich stoichiometries have been observed for this surface.

For the as-deposited 8 nm Co film [Fig. 1(b)] a diffuse (1×1) LEED pattern was observed, which sharpens slightly prior to annealing at 300 °C [Fig. 1(c)], indicating that the Co film grows epitaxially on the SiC substrate. The chemical composition of the surface of the film starts to change [Fig. 1(d)] during annealing at 500 °C. Si and C peaks appear and the characteristic feature of the latter indicates graphitic bonding.[18] This structure shows a $(\sqrt{3}\times\sqrt{3})$ LEED pattern. After annealing at 700 °C a completely diffuse LEED pattern as well as a significant increase of the C peak [Fig. 1(e)] were observed. This suggests that graphitic carbon is forming on the surface of the film.

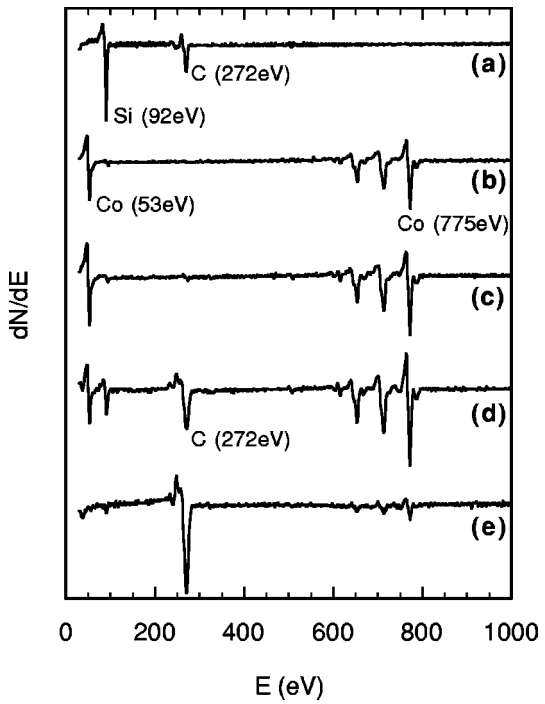

FIG. 1. AES spectra of (a) the $(\sqrt{3}\times\sqrt{3})$ SiC surface, (b) after deposition of 8 nm Co, and after annealing at (c) 300, (d) 500, and (e) 700 °C.

The formation of graphitic carbon is confirmed by XPS measurements of a 1 nm Co film on $(\sqrt{3}\times\sqrt{3})$ SiC annealed stepwise up to 1200 °C. These measurements are depicted in Fig. 2. The C 1*s* peak of the uncoated SiC [Fig. 2(a)] displayed only a Si-bonded state located at 283.4 eV. The deposition of 1 nm Co causes a peak shift to 283.1 eV resulting from the Schottky barrier at the Co/SiC interface. After annealing at 630 °C, a shoulder appears at 284.5 eV attributed to C-C bonds.[19] This is in agreement with the literature, which also reports the formation of carbon or graphite on the surface of Co on SiC.[2,6,20] After annealing at 1200 °C, the XPS signal of the Co and the C shoulder vanish. This indicates that the Co has evaporated from the surface and apparently the graphitic carbon is removed during this process [Fig. 2(b)].

The most remarkable feature of Fig. 2(b) is that the Co 2*p* peaks (the $2p_{3/2}$ is located at 778.4 eV) do not shift to higher energies even after annealing at 1000 °C, suggesting that the film still consists mostly of unreacted Co metal (a reference spectrum for $CoSi_2$ is given in Fig. 5 below). However, a small shoulder on the lower-binding-energy side of the Si 2*p* peak of SiC in Fig. 2(c) indicates that a small amount of cobalt silicide does form after annealing at 630 °C. Whether it is Co_2Si, CoSi, or $CoSi_2$ is not clear. This shoulder also vanishes after evaporation of the Co film at 1200 °C.

The local structure of the directly deposited Co films was studied by XAFS. The Fourier transform of the XAFS data for 8 and 2 nm Co films on $(\sqrt{3}\times\sqrt{3})$ SiC annealed at 700 °C as well as standard spectra for Co metal and $CoSi_2$ are shown in Fig. 3. These spectra indicate mainly Co-Co bonds for the directly deposited Co films on $(\sqrt{3}\times\sqrt{3})$ SiC in agreement with the XPS measurements. From a fit of the x-ray absorp-

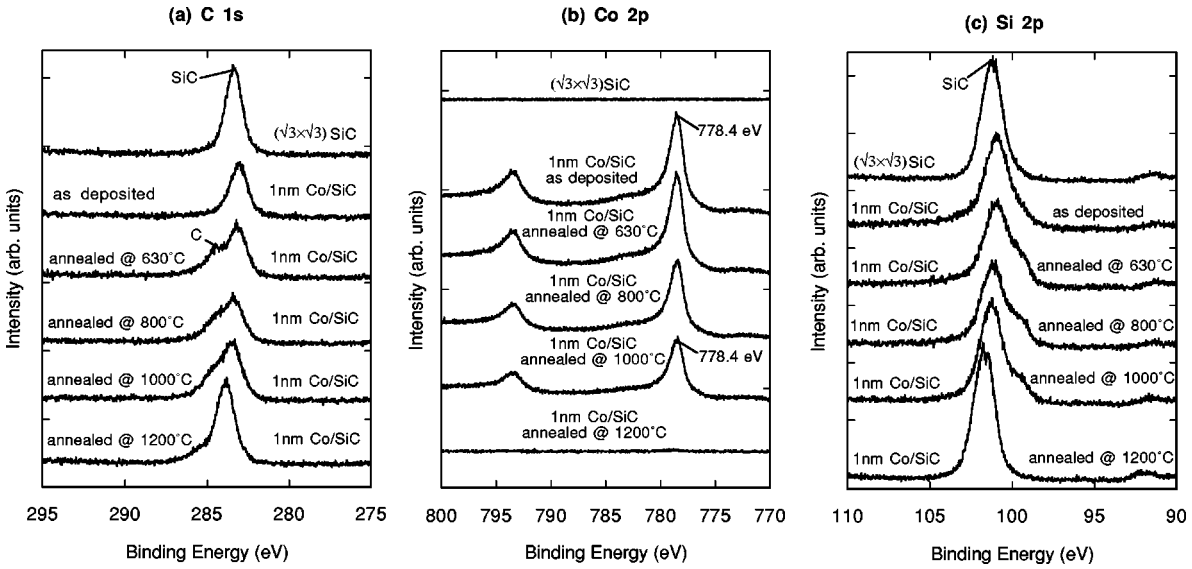

FIG. 2. XPS (a) C 1*s*, (b) Co 2*p*, and (c) Si 2*p* photoelectron peaks from the $(\sqrt{3}\times\sqrt{3})$ SiC surface, after deposition of 1 nm Co at room temperature and after annealing at 630, 800, 1000, and 1200 °C.

tion near edge spectra (XANES), we estimate that the films consist of 70% Co metal and 30% $CoSi_2$. Similar results were obtained by our group for Co films directly deposited on $(1\times1)6H$-SiC(0001).[7] For 2.5 and 10 nm Co films annealed at 800 °C, only Co-Co bonds due to unreacted Co metal were identified. It might be possible that an interfacial silicide layer forms, which could act as a barrier for further C surface diffusion and thus stop the supply of Si atoms.

Shown in Fig. 4 are *ex situ* AFM data collected from the Si-etched 6*H*-SiC(0001) and from an 8 nm Co film deposited on this surface and annealed at 700 °C. The 6*H*-SiC(0001) surface showed an ordered $(\sqrt{3}\times\sqrt{3})$-*R*30° LEED pattern before it was taken out of the UHV system. Mechanical scratches, typical of polishing, can be seen [Fig. 4(a)] running irregularly across the surface (see also Refs. 21 and 22). The root-mean-square (rms) roughness measured from the image is 2.15 nm. Since these polishing scratches were also observed for the as-supplied 6*H*-SiC(0001) covered by native oxides and other contaminants, it can be concluded that the UHV Si molecular beam etching does not affect this mechanical damage, which is in agreement with prior studies.[22] The 8 nm Co film deposited on this surface replicates the polishing scratches of the underlying 6*H*-SiC(0001), giving a rms roughness of 1.6 nm.

Nathan and Ahearn[8] studied Co films (5–20 nm) directly deposited on amorphous SiC (10 nm thick). Rapid thermal annealing revealed the formation of CoSi after annealing at temperatures above 600 °C. Lundberg, Zetterling, and Östling[2] found that 180 nm Co directly deposited on 6H-SiC started to form Co_2Si at 600 °C, CoSi at 900 °C, and $CoSi_2$ at 1100 °C. On the other hand, Porter *et al.*[6] reported the formation of CoSi for 100 nm Co/6*H*-SiC annealed at 1000 °C for 2 min. In a more recent study by Park *et al.*,[9] 25 nm of cobalt deposited on amorphous SiC (200 nm) were annealed over a temperature range from 600 to 1000 °C. The authors found that Co_2Si and CoSi formed at 600 and 800 °C, respectively.

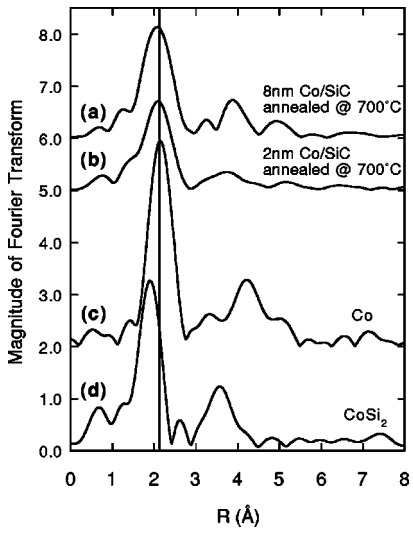

FIG. 3. Fourier transform of k^2-weighted XAFS data for (a) 8 and (b) 2 nm Co on $(\sqrt{3}\times\sqrt{3})$ SiC after annealing at 700 °C, (c) Co foil, and (d) $CoSi_2$.

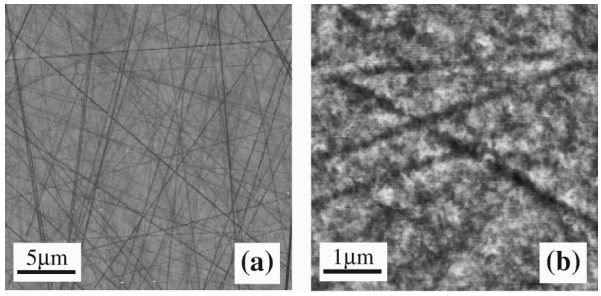

FIG. 4. AFM scans of the $(\sqrt{3}\times\sqrt{3})$ SiC surface (a) before and (b) after direct deposition of 8 nm Co annealed at 700 °C. The scan sizes are 20×20 and 5×5 μm^2, and black-to-white scales are 17 and 11 nm, respectively.

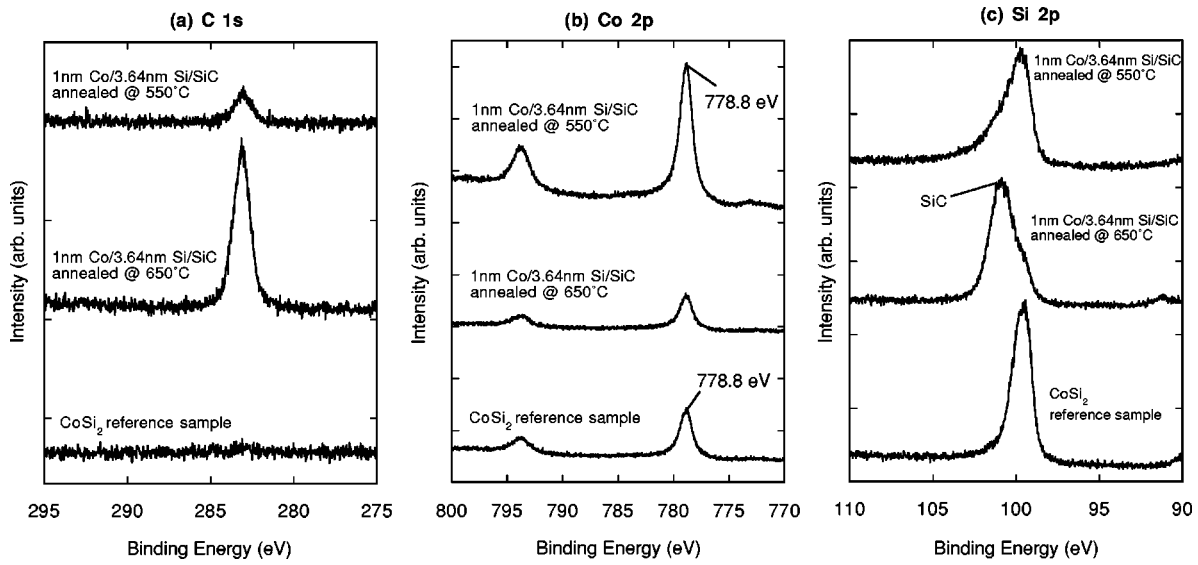

FIG. 5. XPS (a) C 1*s*, (b) Co 2*p*, and (c) Si 2*p* photoelectron peaks from sequentially deposited 1 nm Co/3.64 nm Si on $(\sqrt{3}\times\sqrt{3})$ SiC annealed at 550 and 650 °C. For comparison, $CoSi_2$ is shown.

Co-Si-C ternary phase diagrams proposed by Lundberg and Östling[5] and Schuster[23] at 1350 and 1000 °C, respectively, show that no ternary phase exists. Tie lines connect C with Co_2Si and CoSi as well as SiC with CoSi and $CoSi_2$. Thus, SiC coexists with CoSi and $CoSi_2$, whereas C does not coexist with $CoSi_2$.

The fact that we found mainly unreacted Co metal even after annealing at 1000 °C may be due to the thickness of our films (1–8 nm), which evaporate at lower temperatures (1200 °C) than thick films, and/or the crystallinity and surface reconstruction of the 6*H*-SiC(0001) substrate. It seems that thinner films limit the reaction, as was also reported by Porter *et al.*[6] and Porto *et al.*[7] In addition, in amorphous SiC about 20% of the bonds are homopolar Si-Si bonds, which are weaker than the heteropolar Si-C bonds present in crystalline SiC,[24] favoring the formation at lower temperatures of the cobalt silicides.

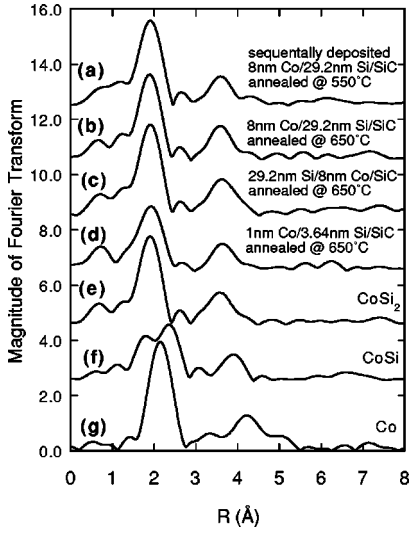

FIG. 6. Fourier transform of k^2-weighted XAFS data for 8 nm Co/29.2 nm Si sequentially deposited on $(\sqrt{3}\times\sqrt{3})$ SiC after annealing at (a) 550 °C, (b) 650 °C, (c) with reversed sequence (annealed at 650 °C), (d) 1 nm Co/3.64 nm Si/$(\sqrt{3}\times\sqrt{3})$ SiC annealed at 650 °C, (e) $CoSi_2$, (f) CoSi, and (g) Co foil.

B. Sequential deposition, codeposition, and template method

Several samples were prepared by sequentially depositing Si and Co with a thickness ratio of 3.64:1 onto the 6*H*-SiC(0001) substrate with a $(\sqrt{3}\times\sqrt{3})$ surface reconstruction. Figure 5 shows the XPS spectra measured from a 1 nm Co/3.64 nm Si bilayer on $(\sqrt{3}\times\sqrt{3})$ SiC after annealing at 550 and 650 °C. Also included in Fig. 5 is a $CoSi_2$ reference sample prepared by depositing 1 nm Co on Si(001) and subsequently annealing at 600 °C. Figure 5(a) shows the C 1*s* peak originating from the SiC substrate, which is relatively smaller than the one for the directly deposited 1 nm Co film [Fig. 2(a)] due to screening effects of the additional 3.64 nm Si. No shoulder on the higher-binding-energy side of this peak appears, i.e., no graphitic bonding is detected. After annealing at 650 °C the C 1*s* SiC peak increases by a factor of 5, suggesting that the film has broken into islands.

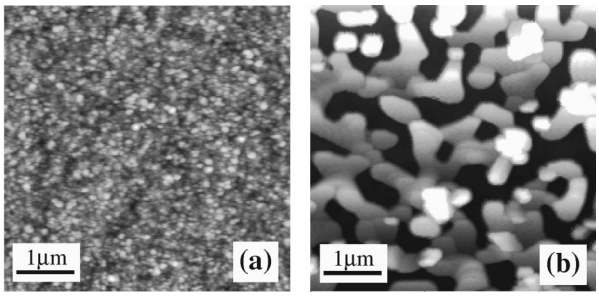

FIG. 7. AFM scans of sequentially deposited 8 nm Co/29.2 nm Si annealed at (a) 550 and (b) 650 °C. The scan size in both cases is 5×5 μm^2. The black-to-white scales are 178 and 119 nm, respectively.

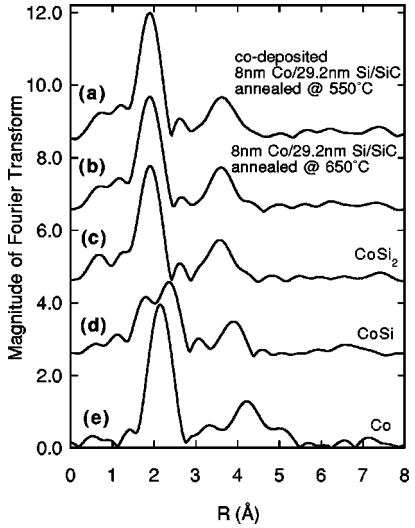

FIG. 8. Fourier transform of k^2-weighted XAFS data for 8 nm Co/29.2 nm Si codeposited on $(\sqrt{3}\times\sqrt{3})$ SiC after annealing at (a) 550 and (b) 650 °C, (c) $CoSi_2$, (d) CoSi, and (e) Co foil.

The results of Fig. 5(b) show that after annealing of the bilayer at 550 °C the Co $2p_{3/2}$ peak shifts to 778.8 eV in comparison to the as-deposited 1 nm Co/SiC [Fig. 2(b)], which has the same binding energy as measured for the $CoSi_2$ reference sample. This observation suggests that the whole bilayer has transformed to cobalt disilicide (3.49 nm). The decrease of the Co $2p$ peaks after annealing at 650 °C is also consistent with islanding of the film. The Si $2p$ peak [Fig. 5(c)] confirms the results of the C $1s$ and Co $2p$ peaks. The main peak for the 550 °C bilayer is at the same binding energy position as in the $CoSi_2$ reference sample, and the SiC peak appears as a shoulder on the higher-energy side. After annealing at 650 °C exactly the opposite situation is found. The silicide peak appears as a small shoulder on the lower-energy side of the SiC peak. This increase of the Si peak is because large parts of the substrate surface are exposed to the x-ray beam due to island formation.

The transformation of bilayers in the thickness range 1 nm Co/3.64 nm Si to 8 nm Co/29.2 nm Si into (3.5–28)-nm-thick $CoSi_2$ films during annealing at 550 or 650 °C is unambiguously shown by the XAFS data in Fig. 6. The bilayers show the same features in the Fourier transform as the $CoSi_2$ reference sample, ruling out the possibility that the films contain significant amounts (>5%) of CoSi or Co metal. The appearance of the higher shells indicates the presence of long-range order. The LEED pattern of the bilayer annealed at 550 °C was diffuse, indicating that this film consists of grains smaller than the correlation length for LEED of 10 nm. In addition, Fig. 6(c) shows that changing the deposition sequence has no effect.

As suggested by the XPS and XAFS data, bilayers annealed at 550 °C form smooth $CoSi_2$ films, but during annealing at 650 °C they break up into islands. AFM images (Fig. 7) showing the surface morphology of these two cases confirm these findings. The surface of the bilayer sample prepared by annealing at 550 °C appears smooth with a small rms roughness of 2 nm. As was the case for the directly deposited Co films [Fig. 4(b)], the surface replicates the polishing scratches of the underlying SiC substrate as observed in larger-scale $20\times20\ \mu m^2$ images (not shown here). In contrast, the bilayer annealed at 650 °C [Fig. 7(b)] is no longer uniform. Islands are observed to form with large substrate regions not covered by the $CoSi_2$ film. The rms roughness of this film is significantly increased to 35 nm. The appearance of a $(\sqrt{3}\times\sqrt{3})$-$R30°$ LEED pattern measured for this sample confirms the AFM data, and, in addition, indicates that the $(\sqrt{3}\times\sqrt{3})$ surface reconstruction is in equilibrium with $CoSi_2$ on the surface.

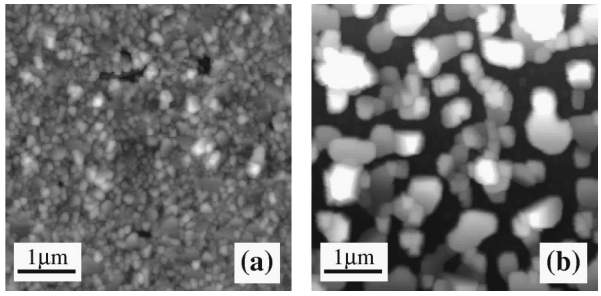

FIG. 9. AFM scans of 8 nm Co/29.2 nm Si codeposited on $(\sqrt{3}\times\sqrt{3})$ SiC and annealed at (a) 550 and (b) 650 °C. The scan size is $5\times5\ \mu m^2$. The black-to-white scales are 91 and 211 nm, respectively.

As expected, films prepared by codepositing Co and Si in a 1:3.64 ratio onto the $(\sqrt{3}\times\sqrt{3})$ SiC surface do form $CoSi_2$. This is indicated by our XAFS measurements depicted in Fig. 8. The spectra of the codeposited films annealed at 550 and 650 °C show the same features as the $CoSi_2$ reference sample. They break up into islands as well when annealed at 650 °C as shown by AFM data in Fig. 9(b), but, in addition, films annealed at 550 °C exhibit a slightly degraded surface morphology, as seen by the formation of pinholes that appear

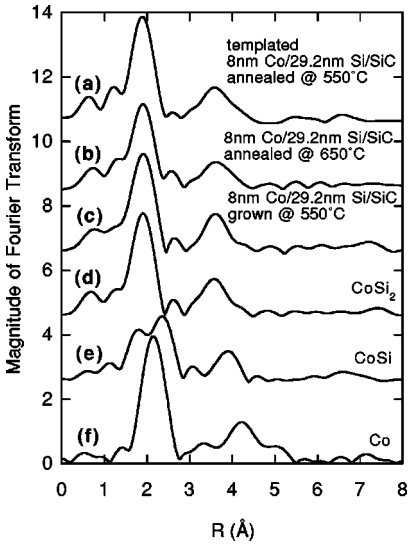

FIG. 10. Fourier transform of k^2-weighted XAFS data for 8 nm Co/29.2 nm Si codeposited on a layered template at 400 °C after annealing at (a) 550 and (b) 650 °C, (c) codeposited on a layered template at 550 °C, (d) $CoSi_2$, (e) CoSi, and (f) Co foil.

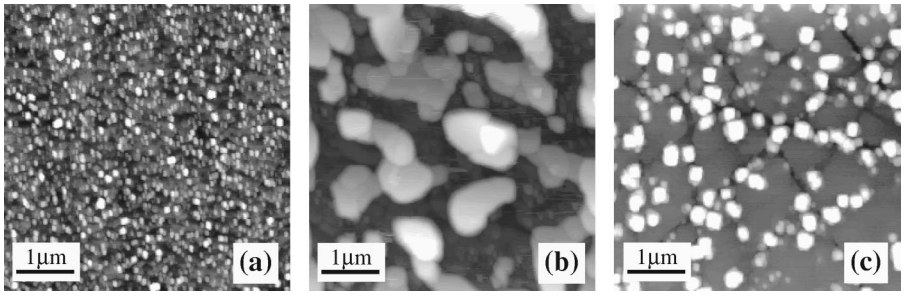

FIG. 11. AFM scans of 8 nm Co/29.2 nm Si codeposited on a layered template at 400 °C and annealed at (a) 550 and (b) 650 °C. The film in (c) was grown on the layered template at 550 °C. The scan size is 5×5 μm^2. The black-to-white scales are 32, 155, and 77 nm, respectively.

to penetrate the entire silicide film [Fig. 9(a)]. The rms roughness of the $CoSi_2$ film annealed at 550 °C is 12 nm, i.e., a factor of 5 higher than for the sequentially deposited film [Fig. 7(a)]. The rms roughness of the film annealed at 650 °C [Fig. 9(b)] is 48 nm, which is comparable to that of the sequentially deposited film annealed at the same temperature [Fig. 7(b)].

To suppress the formation of pinholes and to improve the surface morphology of the codeposited film, the nucleation of $CoSi_2$ on the $(\sqrt{3}\times\sqrt{3})$ SiC surface was controlled through the use of $CoSi_2$ template layers. Template layers were successfully used by our group for the formation of smooth $CoSi_2$ films on SiGe(001), reducing Ge segregation and achieving a rms roughness of 1.5 nm.[25] In this work, the same template structure was used, consisting of 2 ML Si/1 ML Co/2 ML Si deposited at room temperature on the $(\sqrt{3}\times\sqrt{3})$ SiC surface, capped with a stoichiometrically codeposited film of 0.2 nm Co and 0.73 nm of Si. The silicide layer was thickened further by codepositing 8 nm Co and 29.2 nm Si at 400 °C. One sample prepared in this way was subsequently annealed at 550 °C and another one at 650 °C. A third sample was prepared by growing the silicide layer by codepositing 8 nm Co and 29.2 nm Si at 550 °C, i.e., at the maximum temperature before islanding occurs. All three films were investigated with XAFS (Fig. 10). These films show the same features as the $CoSi_2$ reference sample, indicating the transformation into $CoSi_2$. The surface morphology of the three films is depicted in Figs. 11(a)–11(c). The surface of the sample prepared by the template method at 400 °C and subsequently annealed at 550 °C appears rather smooth with a rms roughness of 5 nm, which is about a factor of 2 less than the rms roughness of the surface of the directly codeposited film annealed at the same temperature [Fig. 9(a)]. However, in comparison to the sequentially deposited film annealed at 550 °C [Fig. 7(a)], this surface [Fig. 9(a)] is rougher by more than a factor of 2. Annealing at higher temperatures (650 °C) again leads to islanding as shown in Fig. 11(b). For this surface, morphology and rms roughness (42 nm) are comparable to those of Figs. 7(b) and 9(b).

The surface of the sample prepared by the template method at the maximum temperature (550 °C) before islanding occurs [Fig. 11(c)] shows interesting features. The rms roughness is 14 nm, somewhat larger than that of the film in Fig. 11(a); however, it appears that $CoSi_2$ is agglomerating at the polishing scratches forming chains of $CoSi_2$ clusters, whereas areas between those chains are virtually featureless. The ratio between the average volume occupied by the clusters and that of $CoSi_2$ evaluated from the total of Co and Si deposited is 1:4. In addition, no C peak originating from the SiC substrate was detected with AES for this film. These facts and Fig. 10 show that the areas between the cluster chains also consist of $CoSi_2$. Unfortunately, for films prepared with the template method no LEED was available. However, the featureless areas may be epitaxial silicides. Thus, it might be possible to suppress the agglomeration by removing the polishing scratches with H_2 etching[22] prior to preparing the $(\sqrt{3}\times\sqrt{3})$ SiC reconstruction and the silicide films.

The formation of $CoSi_2$ in the sequentially and codeposited Co/Si films on 6*H*-SiC(0001) as well as in films prepared by the template method is consistent with the Co-Si-C ternary phase diagrams proposed by Lundberg and Östling[5] and Schuster[23] at 1350 and 1000 °C, respectively. These show tie lines between $CoSi_2$ and SiC, i.e., both phases coexist at those temperatures.

IV. SUMMARY

We have studied the structure, chemistry, and morphology of cobalt silicide films on the $(\sqrt{3}\times\sqrt{3})$-*R*30° reconstruction of the Si-terminated surface of 6*H*-SiC(0001). Co films in the thickness range of 1–8 nm were directly deposited on the $(\sqrt{3}\times\sqrt{3})$ SiC surface. Films annealed up to 1000 °C still contain mainly Co metal while graphitic carbon is detected on the film surface. At 1200 °C the Co films evaporate from the SiC surface. Polycrystalline silicide films in the thickness range of 3.5–28 nm were grown by sequential and codeposition as well as by codeposition on template layers. By annealing at 550 °C these films form $CoSi_2$ without C segregation. Further annealing at 650 °C leads to the formation of islands leaving large areas of the underlying $(\sqrt{3}\times\sqrt{3})$ SiC substrate uncovered. The smallest rms roughness (2 nm) was found for the sequentially deposited films, mirroring the polishing scratches of the SiC substrate. For codeposited films annealed at 550 °C we also observed pinholes. The use of template layers did not improve the overall morphology of the $CoSi_2$ films. We observed agglomeration of $CoSi_2$ clusters located at the polishing scratches and large, virtually featureless areas between these cluster chains. If the polishing scratches can be eliminated it may be possible using this template method and low-temperature annealing to produce high-quality, epitaxial contacts on SiC.

ACKNOWLEDGMENTS

The authors would like to thank R. F. Davis for placing the XPS chamber at their disposal. Funding for this work was provided by the Department of Energy under Contract Nos. DE-FG05-93ER79236 (D.E.S., instrumentation) and DE-FG05-89ER45384 (D.E.S., X-11 operations at NSLS), and by the National Science Foundation under Contract No. DMR-9633547 (R.J.N.). The authors gratefully acknowledge use of beamline X-11 at the National Synchrotron Light Source. The NSLS is funded by the Department of Energy under Contract No. DE-AC02-76CH00016.

[1] *SiC Materials and Devices*, Vol. 52 of *Semiconductors and Semimetals*, edited by Y. S. Park (Academic, San Diego, 1998).
[2] N. Lundberg, C.-M. Zetterling, and M. Östling, Appl. Surf. Sci. **73**, 316 (1993).
[3] N. Lundberg and M. Östling, Phys. Scr. **T54**, 273 (1994).
[4] N. Lundberg and M. Östling, Solid-State Electron. **38**, 2023 (1995).
[5] N. Lundberg and M. Östling, Solid-State Electron. **39**, 1559 (1996).
[6] L. M. Porter, R. F. Davis, J. S. Bow, M. J. Kim, and R. W. Capenter, J. Mater. Res. **10**, 26 (1995).
[7] A. O. Porto, B. I. Boyanov, D. E. Sayers, and R. J. Nemanich, J. Synchrotron Radiat. **6**, 188 (1999).
[8] N. Nathan and J. S. Ahearn, J. Appl. Phys. **70**, 811 (1991).
[9] S. W. Park, Y. I. Kim, J. S. Kwak, and H. K. Baik, J. Electron. Mater. **26**, 172 (1997).
[10] U. Starke, Phys. Status Solidi B **202**, 475 (1997).
[11] A. O. Porto, M. L. O'Brien, D. E. Sayers, and R. J. Nemanich (unpublished).
[12] M. Kitabatake, Mater. Sci. Forum **264-268**, 327 (1998).
[13] C. E. Bouldin, W. T. Elam, and L. Furenlid, Physica B **208-209**, 190 (1995).
[14] U. Starke, J. Schardt, and M. Franke, Appl. Phys. A: Mater. Sci. Process. **65**, 587 (1997).
[15] R. Kaplan, Surf. Sci. **215**, 111 (1989).
[16] V. M. Bermudez, Appl. Surf. Sci. **84**, 45 (1995).
[17] L. I. Johansson, F. Owman, and P. Mårtensson, Phys. Rev. B **53**, 13 793 (1996).
[18] T. Tsukamoto, M. Hirai, M. Kusaka, M. Iwami, T. Ozawa, T. Nagamura, and T. Nakata, Surf. Sci. **371**, 316 (1997).
[19] *Handbook of X-ray Photoelectron Spectroscopy*, edited by J. Chastain (Perkin-Elmer, 1992).
[20] N. Lundberg and M. Östling, Appl. Phys. Lett. **63**, 3069 (1993).
[21] P. Mårtensson, F. Owman, and L. I. Johansson, Phys. Status Solidi B **202**, 501 (1997).
[22] Q. Xue, Q. K. Xue, Y. Hasegawa, I. S. T. Tsong, and T. Sakurai, Appl. Phys. Lett. **74**, 2468 (1999).
[23] J. C. Schuster, Int. J. Refract. Met. Hard Mater. **12**, 173 (1994).
[24] G. Galli, F. Gygi, and A. Catellani, Phys. Rev. Lett. **82**, 3476 (1999).
[25] B. I. Boyanov, P. T. Goeller, D. E. Sayers, and R. J. Nemanich, J. Appl. Phys. **86**, 1355 (1999).